ELSEVIER

Biophysical Chemistry 54 (1995) 279–290

Biophysical Chemistry

Detection of water proximity to tryptophan residues in proteins by single photon radioluminescence

S. Bicknese [a,*], Daniel Zimet [b], Julius Park [a], A.N. van Hoek [a], S.B. Shohet [b], A.S. Verkman [a]

[a] *Departments of Medicine and Physiology, Cardiovascular Research Institute, University of California, San Francisco, CA 94143, USA*
[b] *Laboratory Medicine, University of California, San Francisco, CA 94143, USA*

Accepted 7 November 1994

Abstract

We recently developed a single photon radioluminescence (SPR) technique to measure submicroscopic distances in biological samples [Bicknese et al., and Shahrokh et al., Biophys. J., 63 (1992) 1256–1279]. SPR arises from the excitation of a fluorophore by the energy deposited from a slowing beta decay electron. The purpose of this study was to detect ^3H_2O molecules near tryptophan residues in proteins by tryptophan SPR. To detect small SPR signals, a sample compartment with reflective ellipsoidal optics was constructed, and amplified signals from a cooled photomultiplier were resolved by pulse-height analysis. A Monte Carlo calculation was carried out to quantify the relationship between SPR signal and ^3H_2O–tryptophan proximity. Measurements of tryptophan SPR were made on aqueous tryptophan; dissolved melittin (containing a single tryptophan); native and denatured aldolase; dissolved aldolase, monellin, and human serum albumin; and the integral membrane proteins CHIP28 (containing a putative aqueous pore) and MIP26 using ^3H_2O or the aqueous-phase probe ^{3}H-3-*O*-methylglucose (OMG). After subtraction of a Bremsstrahlung background signal, the SPR signal from aqueous tryptophan (cps $\cdot$ μCi^{-1} μmol^{-1} $\pm$ SE) was 8.6 $\pm$ 0.2 with ^3H_2O and 7.8 $\pm$ 0.3 with ^{3}HOMG ($n = 8$). With ^3H_2O as donor, the SPR signal (cps $\cdot$ μCi^{-1} μmol^{-1}) was 9.0 $\pm$ 0.3 for monomeric melittin in low salt (tryptophan exposed) and 4.6 $\pm$ 0.8 ($n = 9$) for tetrameric melittin in high salt (tryptophans buried away from aqueous solution). The ratio of SPR signal obtained for aldolase under denaturing conditions of 8 M urea (fluorophores exposed) versus non-denaturing buffer (fluorophores buried) was 1.53 $\pm$ 0.07 ($n = 6$). Ratios of SPR signals normalized to fluorescence intensities for monellin, aldolase, and human serum albumin, relative to that for *d*-tryptophan, were 1.42, 1.09, and 1.04, indicating that the cross-section for excitation of fluorophores in proteins is greater than that for tryptophan in solution. For the CHIP28 and MIP26 proteins in membranes, the ratio of SPR signal obtained with ^3H_2O versus ^{3}HOMG was 1.35 $\pm$ 0.13 (CHIP28, $n = 5$) and 0.99 $\pm$ 0.02 (MIP26). These data are consistent with the existence of an aqueous channel through CHIP28 that excludes small solutes. We conclude that tryptophan radioluminescence in proteins is measurable and provides unique information about the presence of local aqueous compartments.

Keywords: Tryptophan; Single photon radioluminescence; Fluorescence; Melittin; CHIP28; Water; Mathematical modeling

1. Introduction

The accessibility of water to tryptophan residues in soluble and integral membrane proteins provides

* Corresponding author.

SSDI 0301-4622(94)00127-8

information about protein structure. The environment and location of tryptophans in proteins have been studied by several biophysical methods which are based on measurement of intrinsic tryptophan fluorescence. The polarity of the tryptophan environment has been examined by fluorescence emission spectra and the accessibility of aqueous-phase quenchers such as iodide and acrylamide [3,4]; the location of tryptophans in membrane proteins has been determined by fluorescence resonance energy transfer (RET) using acceptor molecules that reside at specific depths in the bilayer [5,6]. Probe molecules, such as fluorescence quenchers and energy transfer acceptors, provide indirect data about the proximity of water molecules to tryptophan residues. Probes may perturb protein structure and be excluded from certain aqueous domains because of their size or charge.

We report here a novel biophysical approach to determine the proximity of tritiated water molecules to tryptophan residues in proteins based on single photon radioluminescence (SPR). Because the access of water molecules to tryptophans is measured directly, soluble or membrane proteins can be studied in native conformation without the perturbation or uncertainties introduced by exogenous probes. SPR utilizes the energy deposited by beta decay in the vicinity of a fluorophore to excite an S_0-to-S_1 transition which produces conventional visible or UV fluorescence upon radiative de-excitation [1]. The probability of fluorophore excitation is a function of the distance between the radioactive 'donor' and fluorescent 'acceptor', as well as fluorophore molar absorbance, and under some conditions, fluorophore environment. Fluorophore emission depends on quantum yield and the other factors that apply in conventional fluorescence spectroscopy. The relationship between fluorophore excitation efficiency and donor–acceptor decay in SPR is very different than that in RET and can be exploited to measure long distances (10–100 nm), and as reported here, very short distances (< 1 nm) that are not easily measurable by other techniques.

The purpose of this study was to evaluate the utility of SPR to detect the tryptophan radioluminescence arising from excitation by tritiated water molecules that are very close to tryptophan residues in soluble and membrane proteins. First, a theoretical Monte Carlo calculation was carried out to predict the SPR signal expected in biological samples and to provide a semi-quantitative relationship between water–tryptophan distance and SPR signal. To detect very small SPR signals and signal differences, an improved detection system was constructed that utilized ellipsoidal photon capture optics. SPR was then applied to determine the proximity of tritiated water to tryptophans in the soluble protein melittin, which contains a single tryptophan residue and undergoes salt-dependent aggregation; in the soluble protein aldolase, which exposes a fraction of its tryptophan residues to the aqueous environment when denatured by 8 M urea; in monellin and human serum albumin (HSA) compared to aldolase and *d*-tryptophan; and in the membrane proteins CHIP28, a water channel, and MIP26, a non-water channel homologue of CHIP28. The results demonstrate the utility of SPR to measure very short distances and provide information about the proximity of water to tryptophans in water soluble proteins and a transmembrane water channel.

2. Materials and methods

2.1. Theory

A Monte Carlo calculation was performed to determine the spatial distribution of energy deposited by a beta electron very near a ^{3}H source. The calculation for distances of > 10 nm from the ^{3}H source was described in detail previously [1]. The continuous-slow-down approximation [7] was applied to a series of monoenergetic ^{3}H electrons as a succession of steps, each with a defined energy loss. The initial energies of the electrons were taken at intervals of 0.5 keV for energies of 2–18.5 keV and at intervals of 0.1 keV for energies of 0.5–2 keV. The electron energy at step n (E_n) was equal to $2^{1/m} E_{n-1}$, where m was set to 10^5 to give high resolution for the first 500 steps and 10^3 for remaining steps to deplete the electron energy to < 0.5 keV. The energy loss with distance ($-\mathrm{d}E/\mathrm{d}x$) was calculated according to the relativistic Bethe equa-

tion [8,9] and applied in discreet steps as proposed by Berger [10],

$$S_{n+1} = \left[(1 - 2^{-1/m})E_n + S_n\langle dE/dx\rangle\right]/\langle dE/dx\rangle \quad (1)$$

where $\langle dE/dx\rangle$ is the average energy loss over the interval between positions S_{n+1} and S_n as calculated by the Bethe equation, m is the number of steps required to deposit half of the electron energy and E_n is electron energy at S_n. At each step, the electron 3-dimensional trajectory was given a random change in direction based on a normal distribution of directions with mean value determined from the absolute energy loss [11]. Electron energy deposition was binned in intervals of 0.01 nm for the first 5 nm and 1 nm thereafter to a maximum electron range of ca. 4 μm. dE/dx for beta electrons having energies below 0.5 keV is not well described by the Bethe equation, but their range is predicted to be very small. Energy from these electrons was deposited near the ^{3}H molecule according to the distributions provided by Berger [10]. Monte Carlo calculations were carried out for 200 electrons at each initial energy and integrated to give the deposited energy density ($D(R)$, keV/cm^3) as a function of distance (R) from the ^{3}H molecule. The calculation required ca. 100 hours of computational time on a 80486 cpu. In addition, the electron recombination energy of 24.6 eV from the remaining $^3He^+$ ($^3H \rightarrow {}^3He^+ + e^- + \bar{\nu}$) was deposited over a distance of ca. 5 nm as predicted from the $^3He^+$ recoil velocity (15000 m/s) and time for $^3He^+$-electron recombination (ca. 10^{-13} s) [12,13] (Fig. 1A). The SPR signal (L_{rad}, counts per second, cps) in solution, in which ^{3}H molecules are randomly assembled in 3-dimensions around the fluorophore acceptor at the center of a sphere of radius r_c in which ^{3}H is excluded (Fig. 1B), is proportional to the integral of $R^2D(R)$ over $R = r_c$ to ∞. The R^2 term arises from the increasing number of radioisotopes at distance R. The ratio of SPR signals predicted in the absence (L^-_{rad}) versus the presence (L^+_{rad}) of an excluded volume is,

$$L^-_{rad}/L^+_{rad} = \int_0^\infty R^2D(R)\,dR \Big/ \int_{r_c}^\infty R^2D(R)\,dR \quad (2)$$

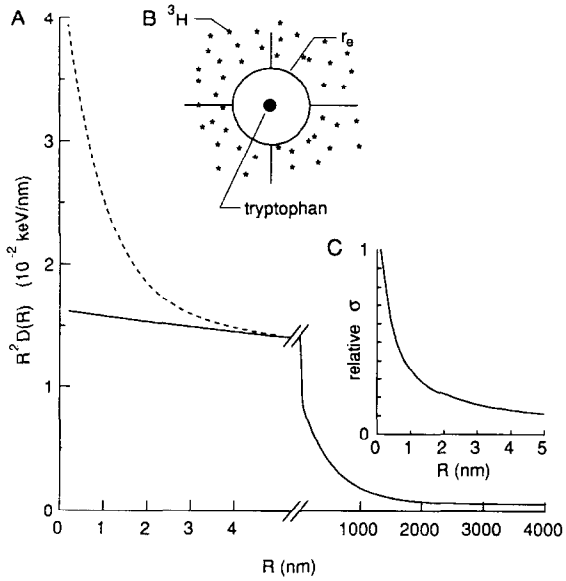

Fig. 1. Monte Carlo calculation of predicted SPR signals. (A) SPR energy deposition (R^2 $D(R)$) by beta electrons (solid line) and ^{3}He$^+$-electron recombination (dashed line) See text for details. (B) Schematic of a single tryptophan surrounded by ^{3}H donors everywhere except for a spherical volume of radius r_c. (C) Cross-section (σ) for dipole excitation by a beta electron as a function of electron energy (E) and range (R); $\sigma \propto E^{-1}$ ln(E)E -1 ln(E) and $R = 40E(1+0.5E)$ [12].

2.2. Instrumentation

The SPR instrument consisted of a photomultiplier in a cooled housing (models 9235QA and Fact-50; Thorn EMI, Rockaway, NJ), high-voltage power supply (model 126; Pacific Instruments, Concord, CA) and signal processing electronics (models 113 preamplifier, 590A pulse shaper and Ace/2K multichannel analyzer card; EG and G-Ortec) as described previously [2]. The instrument was modified for this study by the construction of ellipsoidal photon collection optics. A mirrored (rhodium coated) ellipsoidal chamber was constructed by joining two reflectors (major and minor axes, 16.8 cm and 8.9 cm, Melles-Griot, Irvine, CA) with a 4-cm spacer to complete an ellipsoid with a 14.2-cm interfocal distance. One vertex of the chamber was truncated (shortened by 3.5 cm along the major axis) to mount to the photomultiplier housing with one focus of the ellipsoid positioned near (ca. 2 cm) the photomultiplier window (Fig. 2). A filter holder was positioned between the ellipsoidal chamber and the window of the photomultiplier housing to accommodate 50 × 50

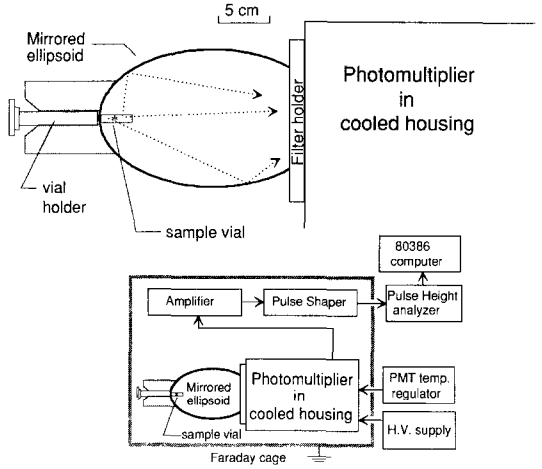

Fig. 2. Schematic of SPR apparatus with ellipsoidal photon collection optics. A rhodium-coated ellipsoidal reflector was mounted on the cooled housing of the photomultiplier so that one focus of the ellipsoid was at the window of the photomultiplier. A 1-ml glass sample vial was positioned at the opposite focus by a Delrin (nylon) holder. Several possible photon paths are shown (dotted lines). The SPR signal was amplified and detected by photon counting electronics and pulse-height discrimination. See text for details.

mm filters of up to 3 mm thickness. A Delrin plastic sample-vial holder was constructed to retrieve a 1-ml sample vial from a storage compartment and position it inside the ellipsoidal chamber at the opposite focus 16.3 cm from the photomultiplier window. The modified chamber and sample holder increased photon capture efficiency by 4.8-fold giving a collection efficiency of 25%; the overall measurement precision increased ca. 10-fold as determined from the standard deviations for repeated measurements on a single sample that was removed and reinserted between measurements. External background signal was reduced by surrounding the instrument with a grounded Faraday cage and performing all measurements in a darkened room. Bremsstrahlung background and other internal sources of background signal (e.g. chemiluminescence) were reduced by placing a cut-on or band-pass filter between the ellipsoidal chamber and the photomultiplier. A UG11 band-pass filter (Schott Glass, Duryea, PA) was used for measurements on aldolase, CHIP28 and MIP26 samples.

2.3. Sample preparation

Radioisotopes and their sources were: $^{3}H_{2}O$ (American Radiolabeled Chemicals, St. Louis, MO) and ^{3}H-3-*O*-methyl glucose (^{3}HOMG) in ethanol (New England Nuclear Research Products, Boston, MA). The ^{3}HOMG was dried before addition to samples. *d*-Tryptophan, melittin and rabbit-muscle aldolase were obtained from Sigma Chemical Co. (St. Louis, MO). *d*-Tryptophan and melittin (1.4 and 0.14 to 0.19 mM) were dissolved in 10 mM sodium phosphate buffer at pH 7.4 containing 0 or 2 M NaCl. To compare fluorophore exposure in the native and denatured states of a soluble protein, aldolase (0.026 mM) was dissolved in 20 mM sodium phosphate buffer at pH 7.4 containing 0 or 8 M urea. To compare fluorophore exposure to water in different proteins, monellin (0.092 mM), HSA (0.125 mM), aldolase (0.036 mM) and *d*-tryptophan (0.150 mM) were dissolved in 20 mM sodium phosphate buffer at pH 7.4. CHIP28 (ca. 5 mg/ml in membranes) was prepared from hemoglobin-free erythrocyte ghosts by stripping twice with 3% N-lauroylsarcosine [14]. CHIP28 was functional as a water channel in this preparation and constituted > 95% of total protein. MIP26 in membranes (ca. 5 mg/ml) was prepared from bovine lens by homogenization followed by successive stripping with 7 M urea and 0.1 M NaOH [14]. MIP26 constituted ca. 80% of the protein in this preparation. CHIP28 and MIP26 protein concentrations were determined by a modified Lowry assay in the presence of SDS.

2.4. Measurement procedures

SPR signal was measured for each sample over three successive periods of 120 s each. Each sample was measured at least twice in this manner in rotation with all other samples to check for drift in instrument sensitivity. Several samples, in addition to the SPR sample (containing radioisotope and fluorophore), were prepared for background subtraction including: an SPR sample blank (containing fluorophore without radioisotope), a Bremsstrahlung sample (containing radioisotope without fluorophore), and a Bremsstrahlung blank (containing no fluorophore or radioisotope). Samples were prepared in parallel, where possible, to ensure equal concen-

trations of fluorophore and radioisotope. The SPR signal arising from fluorophore radioluminescence was corrected (L_{cor}, cps · μCi^{-1} μmol^{-1}) using the equation,

$$L_{cor} = \left\{\left[\left(S_{rad} - Sb_{rad}\right)/S_{\mu Ci}\right] - \left[\left(B_{rad} - Bb_{rad}\right)/B_{\mu Ci}\right]\right\} \cdot \mu mol_{fluor}^{-1}\, Q_y^{-1} \quad (3)$$

where S_{rad} is SPR sample signal (cps), Sb_{rad} is SPR sample blank signal, $S_{\mu Ci}$ is SPR sample radioactivity, B_{rad} is Bremsstrahlung signal, Bb_{rad} is Bremsstrahlung blank signal, $B_{\mu Ci}$ is Bremsstrahlung sample radioactivity, μmol_{fluor} is the molar fluorophore quantity and Q_y is fluorophore quantum yield. The SPR signal was expressed in units of cps · μCi^{-1} μmol_{fluor}^{-1}. Fluorophore concentrations were determined by absorption (Beckmann, model DU-7 spectrophotometer) and radioactivity (μCi) by triplicate scintillation counting of each sample (Beckmann, model LS8000 scintillation counter). SPR data for CHIP28 and MIP26 are reported as ratios of SPR signals obtained from paired samples (containing ^3H_2O or ^{3}HOMG) with identical protein concentration. Fluorophore quantum yield was measured on an SLM 8000C fluorimeter using quinine sulfate in 2.0 M H_2SO_4 as the standard ($Q_y = 0.70$). Quenching of aldolase fluorescence by I^- was measured on an SLM 8000C fluorimeter by adding small aliquots of 5 M KI in 20 mM sodium phosphate buffer (pH 7.4) to a cuvette containing 2 ml of 0.14 μM aldolase. Fluorescence excitation spectra were measured on an SLM8000C using 1:50 dilutions of SPR samples for *d*-tryptophan, aldolase, monellin, and HSA in 20 mM sodium phosphate buffer (pH 7.4). Samples were excited in the range 220–310 nm and detected with a 4911 band pass filter in the emission path. The corrected SPR signal intensity was expressed as a ratio of SPR signal intensity (cps · μCi^{-1} gm^{-1}) to the fluorescence signal integrated over excitation wavelengths (SPR/ΣF_{ex}). Standard errors for L_{cor} or L_{cor} signal ratios are reported for measurements performed on independent samples. Levels of significance for differences were determined by the Student's *t* test.

3. Results

3.1. Theoretical predictions of SPR signal from fluorophores near an ^3H source

Fig. 1A (solid line) shows the spatial distribution of energy deposited by beta electrons (R^2 $D(R)$, keV/nm) in an aqueous environment as determined by Monte Carlo calculation. The energy density ($D(R)$, keV/cm^3) has been multiplied by R^2 to show the decreased deposited energy as a function of distance R in a manner which is independent of the $1/R^2$ point-source term. The integral of R^2 $D(R)$ over $R = 0$ to ∞ gives 5.5 keV, the mean energy of the ^{3}H beta electron. As described in *Methods*, the SPR signal from an ensemble of radioisotope sources surrounding a fluorophore is proportional to the area under the curve. R^2 $D(R)$ as determined from the Monte Carlo calculation (solid line) decreases with R, reaching a half-maximal value at ca. 50 nm. This relatively modest decrease in R^2 $D(R)$ at very small R is not sufficient to account for the reduction in SPR signal observed experimentally (see below) when ^{3}H is excluded from a small volume ($R < 5$ nm) around the fluorophore.

However, there are additional physical processes that must be included for determination of the probability of excitation of a fluorophore very near a ^{3}H source. These processes have direct implications for the SPR signal arising from an ensemble of ^{3}H sources surrounding a tryptophan residue centered within a spherical volume of radius r_e from which ^{3}H is excluded (Fig. 1B). The following is a semi-quantitative description of these physical processes which strongly increase the probability of excitation of a fluorophore very near an ^{3}H source:

(1) *Non-linear dependence of dipole excitation on electron energy:* For fluorophores not very near an ^{3}H source, it was assumed that the probability of fluorophore excitation is proportional to the dipole excitation cross-section, σ, and the energy density deposited by the beta electron at the site of the fluorophore [1]. It was further assumed that σ was a constant property of the fluorophore related to the oscillator strength and independent of fluorophore proximity to the ^{3}H source. However, the Bethe excitation cross-section for inelastically scattered beta electrons, σ_i, is proportional to $A \cdot T^{-1}$ $\ln(T)$, where

T is electron energy and A is related to the ratio of dipole to fluorophore excitation energy [15]. Therefore, fluorophore cross-section is increased for excitation by low-energy short range electrons. Fig. 1C shows that fluorophore excitation probability can increase by 10-fold at a distance of 0.1 nm from the ^3H source compared to distances far from the source. It is also noted that energy deposition in an aqueous environment provides an indirect source of fluorophore excitation and the rate of energy deposition (dE/dx) in liquid water is greatest for low-energy electrons (ca. 100 eV) [12]. Fluorophore excitation probability becomes nearly constant at distances of > 10 nm from the source as assumed in our previous work.

(2) *Energy from $^3He^+$ – electron recombination:* ^3H decay produces an ionized $^3He^+$ which can deposit energy locally to excite radioluminescence. As described in *Methods*, the energy of recombination (24.6 eV/$^3He^+$) will be distributed over a small distance (ca. 5 nm) and will contribute substantially to the energy available for fluorophore excitation (dashed line, Fig. 1A). The precise spatial distribution of this 'recombination' energy cannot be specified because of uncertainties in recombination time; in addition, the theory for dipole excitation cross-section from the energy produced by $^3He^+$ recombination has not been established.

The physical arguments above suggest that enhanced radioluminescence occurs in fluorophores very near a ^3H source because of special physical processes that do not operate at larger distances. In addition, the ionization values used in the Monte Carlo calculation of beta electron energy losses are correct for an aqueous environment and may not accurately model energy losses very close to tryptophans buried within a protein. To test whether tryptophan radioluminescence is measurable and can arise from beta decay of nearby ^3H_2O molecules, experiments were carried out with aqueous tryptophan, melittin, aldolase, albumin and two integral membrane proteins.

3.2. Tryptophan radioluminescence in melittin

The model protein melittin contains a single tryptophan residue. Melittin is present in monomeric form in low-salt buffer in which the tryptophan is exposed at the surface, and in tetrameric form in high-salt buffer in which the tryptophans are buried [16]. Melittin (140–200 μM) was dissolved in 10 mM sodium phosphate buffer (pH 7.4) with or without 2 M NaCl. ^3H_2O (ca. 50 μCi/ml) was used as the SPR donor. At low salt, the single tryptophan in monomeric melittin is exposed to the aqueous environment as demonstrated by the red-shifted fluorescence spectrum with the emission peak at 350 nm (Fig. 3A). The corrected tryptophan SPR signal from melittin and ^3H_2O at low salt was 9.0 ± 0.3 cps · μCi^{-1} μmol^{-1} tryptophan (SE, $n = 6$ separate samples) after correction for measured quantum yield of 0.13 (Fig. 3B). This value is not significantly different from the corrected SPR signal of 8.6 ± 0.2 cps · μCi^{-1} μmol^{-1}, ($n = 4$, quantum yield 0.19) obtained for 1.4 mM *d*-tryptophan dissolved in the same buffer and exposed to ^3H_2O. These results support the conclusion that the single tryptophan in the melittin molecule is exposed to the aqueous environment [17]. At high salt, melittin assumes a 65% α-helical secondary structure and self-associates as tetramers in which the tryptophan of each monomer is buried at the center of the tetramer. The blue shift in the tryptophan emission peak to 330 nm for melittin in high salt (Fig. 3A) demonstrates that the tryptophan residues are shielded from the aqueous environment. The tryptophan SPR signal for melittin in high salt with ^3H_2O was 4.6 ± 0.8 cps · μCi^{-1} μmol^{-1} ($n = 6$) after correction for the quantum yield of 0.25 (Fig. 3B). The predicted geometry of the melittin tetramer in the putative α-helical form suggests that ^3H_2O is excluded from a volume around the buried tryptophans with a radius of 15 Å. This significant decrease in SPR signal arising from the melittin tetramer compared with the monomer ($p < 0.01$) is consistent with the exclusion of ^3H_2O from the vicinity of the tryptophan residue and the consequent decrease in energy density (see *Discussion*).

3.3. Tryptophan radioluminescence in aldolase

Rabbit-muscle aldolase is a water soluble tetrameric protein containing 12 tryptophans and 44 tyrosines [18]. In the 20 mM sodium phosphate buffer, the tryptophans in aldolase are shielded from the aqueous environment as shown by the blue shift

(322 nm) of its fluorescence emission peak (Fig. 4A). Addition of 8 M urea caused a red shift (346 nm) of the aldolase fluorescence emission peak (Fig. 4A), indicating exposure of one or more tryptophans to an aqueous environment. The tryptophan environment was investigated further by measurement of tryptophan quenching by iodide. The Stern–Volmer

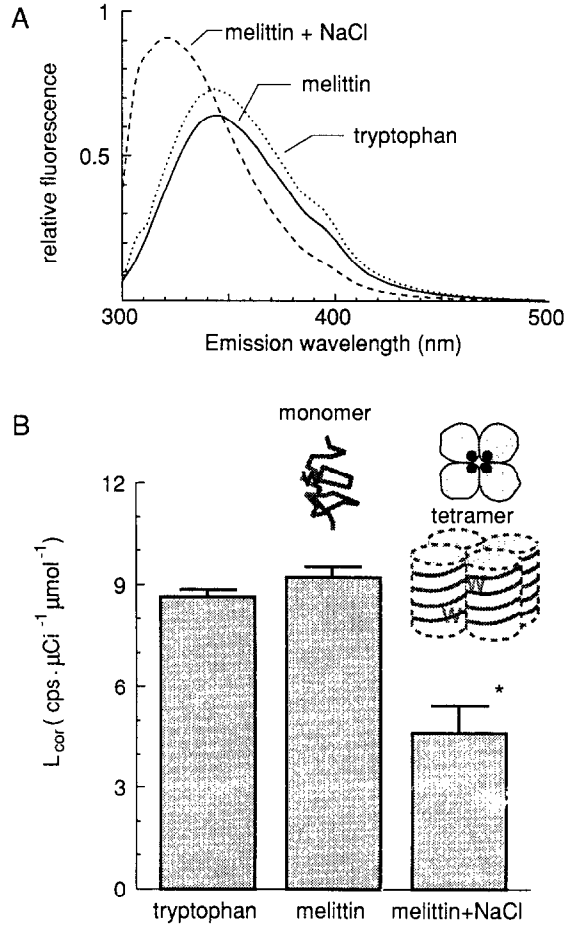

Fig. 3. Fluorescence spectra and SPR signal for *d*-tryptophan and melittin in high- and low-salt solutions. (A) Corrected fluorescence emission spectra of *d*-tryptophan (0.14 mM) and melittin (0.18 mM) in 10 mM sodium phosphate buffer (pH 7.4) containing 0 or 2 M NaCl. (B) Tryptophan SPR signal (L_{cor} + SE, cps·μCi^{-1} μmol^{-1}) from *d*-tryptophan (1.4 mM, $n = 4$) and melittin (0.14–0.19 mM, $n = 6$) in 10 mM sodium phosphate buffer (pH 7.4) containing 0 or 2 M NaCl with ^3H_2O as donor. (*) indicates significant difference from aqueous tryptophan and low-salt melittin ($p < 0.01$). Schematic of monomeric and tetrameric melittin showing exposed and buried tryptophans (W) is provided above the data bars.

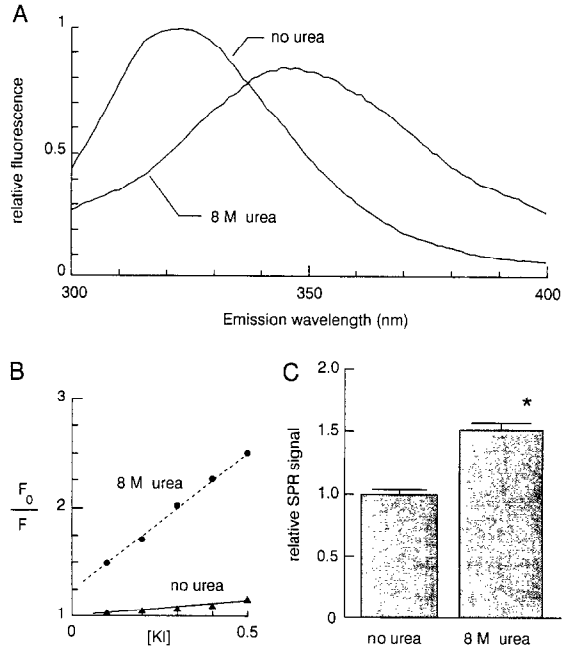

Fig. 4. Fluorescence spectra, Stern–Volmer quenching and SPR signal ratios for rabbit-muscle aldolase. (A) Corrected fluorescence emission spectra (excitation 280 nm) for native and denatured aldolase (0.14 μM) in 20 mM sodium phosphate buffer (pH 7.4) with 0 or 8 M urea. (B) Stern–Volmer plot of fluorescence quenching by KI for native and denatured aldolase in 20 mM sodium phosphate buffer containing 0 or 8 M urea where F_0 and F are the integrated fluorescence under non-denaturing and denaturing conditions with excitation at 280 nm. (C) SPR signal (L_{cor} + SE, cps·μCi^{-1} μmol^{-1} protein) from native and denatured aldolase (25 μM) in 20 mM sodium phosphate buffer containing 0 or 8 M urea with ^3H_2O as donor. SPR signal is corrected for relative fluorescence. (*) indicates significant difference in SPR signal ($p < 0.005$).

constant, K_D, for quenching of aldolase tryptophan fluorescence in the non-denaturing buffer was 0.31 M^{-1} and was substantially increased under denaturing conditions with urea (Fig. 4B). Non-linearity and an intercept > 1 for the Stern–Volmer plot of quenching data in the presence of 8 M urea suggested that only a fraction of the tryptophan residues becomes exposed to the aqueous environment. A plot of $F_0/(F_0 - F)$ versus $1/[KI]$ (based on the modified Stern–Volmer equation $F_0/(F_0 - F) = (1/[KI])\ f_a K_D + 1/f_a$, [19]) provided a better fit of quenching data with urea; the fitted values were 11.2 for K_D and 0.64 for f_a, the fraction of fluorescent residues that were quenched (not shown). Because

the presence of multiple tryptophan and tyrosine residues in aldolase prevented a simple correction of SPR values for quantum yield, excitation spectra were measured for the SPR samples (0 and 8 M urea) by cuvette fluorimetry using the same band-pass filter (UG11) in the emission path as was used in the SPR instrument (data not shown). Excitation was by light wavelengths of 220–310 nm to approximate the wide range of excitation energies in SPR. The integrated spectra showed that total fluorescence intensity in the non-denatured aldolase was 95% of that in the denatured sample, providing a small correction factor for the total relative fluorescence of each sample. The ratio of corrected SPR signal from aldolase and ^3H_2O in denaturing conditions versus aldolase and ^3H_2O under non-denaturing conditions was 1.53 ± 0.07 ($n = 6$) (Fig. 4C). The significant increase in SPR signal arising from the denatured aldolase compared to native aldolase ($p < 0.005$) is consistent with a closer approach of ^3H_2O to tryptophan residues exposed to the aqueous environment.

3.4. Water accessibility of fluorophores in aldolase, monellin and human serum albumin

Monellin and HSA are water soluble proteins, each containing one tryptophan and 7 and 17 tyrosines, respectively. The fluorescence emission maxima of monellin and HSA were blue shifted as compared to *d*-tryptophan (Table 1) indicating that the fluorophores are in a relatively non-polar environment. The Stern–Volmer constants for fluorescence quenching by iodide given in Table 1 support the conclusion that fluorophores in monellin and HSA have an 'aqueous accessibility' between that of *d*-tryptophan and aldolase. For SPR measurements, ^3H_2O (120–140 μCi/ml) was added to monellin, HSA, aldolase and *d*-tryptophan dissolved in 20 mM sodium phosphate buffer. Corrected SPR signals and integrated fluorescence excitation data (ΣF_{ex}) were used to calculate normalized SPR signal ratios as described in *Methods*. This calculation corrects SPR values for the 'average' quantum yield of fluorophores in each protein and facilitates comparison (to tryptophan) of protein fluorophore exposure to ^3H_2O as measured by SPR.

Table 1
Water accessibility of fluorophores in monellin, HSA and aldolase

	Emission maxima (nm)	Stern–Volmer constants (M^{-1})	SPR/ΣF_{ex}
Tryptophan	350	12	1
Monellin	334	5.0	1.42 ± 0.06
HSA	324	7.0	1.04 ± 0.05
Aldolase	314	0.8	1.09 ± 0.05

Emission maxima for monellin, HSA, and aldolase represent the emission wavelength corresponding to maximum fluorescence measured with an excitation wavelength of 280 nm. Stern–Volmer quenching constants for protein fluorescence quenching by NaI (0.1–0.5 M). The ratios of SPR to fluorescence excitation data (SPR/$\Sigma F_{ex} \pm$SD, $n = 3$, see *Methods*) are normalized for comparison to that of tryptophan.

The normalized ratios reported in Table 1 (SPR/$\Sigma F_{ex} \pm$ SE) were expected to be < 1 for proteins because of the relative inaccessibility of protein fluorophores to ^3H_2O causing lower SPR signals compared to *d*-tryptophan. However, ratios > 1 indicated higher SPR cross-sections for protein fluorophore excitation that are not predicted from SPR measurements of *d*-tryptophan in solution (see *Discussion*). Fluorophores in aldolase are isolated from the polar water environment as shown by the blue shift of the emission maximum and the Stern–Volmer constant for quenching by iodide. The observed ratio represents a combination of 2 competing effects: decreased accessibility of ^3H_2O to the fluorophore and increased fluorophore cross-section for excitation by SPR. Fluorophores in monellin and HSA are intermediate in water accessibility compared to aldolase and tryptophan. For HSA, the increased cross-section again balances the decreased accessibility giving a ratio that is not significantly different than 1. However, for monellin, the ratio is significantly greater than 1 ($p < 0.05$), indicating that the increase in cross-section has a greater effect upon SPR signal than the decrease in fluorophore accessibility to ^3H_2O excitation.

3.5. Tryptophan radioluminescence in two integral membrane proteins

Access of ^3H_2O to tryptophan residues in proteins was investigated in two homologous integral membrane proteins: CHIP28 and MIP26. CHIP28 is a water-selective channel protein containing four tryp-

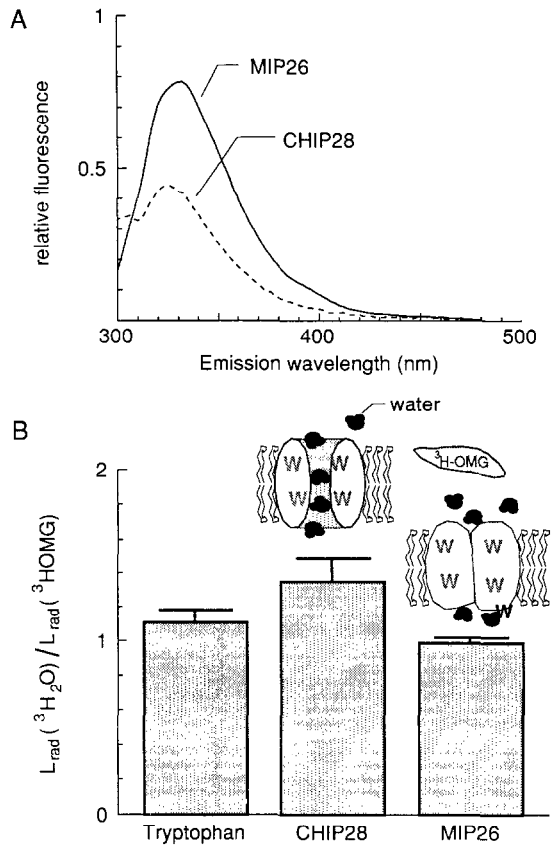

Fig. 5. Fluorescence spectra and SPR signal ratios for *d*-tryptophan and integral membrane proteins CHIP28 and MIP26. (A) Corrected fluorescence emission spectra for CHIP28 (0.5 mg/ml) in N-lauroylsarcosine stripped erythrocyte vesicles and MIP26 (1.0 mg/ml) in stripped bovine lens vesicles. (B) Ratio of corrected SPR signal obtained for ^3H_2O versus ^{3}H-3-*O*-methyl glucose as donor. Schematic of CHIP28 (with water channel) and MIP26 (without water channel) in membranes with SPR donors is shown above the data bars.

tophans that are isolated from the aqueous environment as demonstrated by the blue shift in tryptophan fluorescence (Fig. 5A). MIP26 contains five tryptophan residues and does not function as a water channel (see *Discussion*). The slight blue shift in MIP26 fluorescence (Fig. 5A) suggests that one tryptophan is exposed to the aqueous environment whereas the other four are located in the protein interior [20]. Experiments were carried out to determine whether ^3H_2O in the putative CHIP28 aqueous pore could excite radioluminescence in tryptophans near (but not directly lining) the pore. The relative SPR signal of CHIP28 (10–50 μM in N-lauroylsarcosine stripped vesicles) with ^3H_2O versus ^{3}HOMG as donor was 1.35 $\pm$ 0.13 ($n = 3$) (Fig. 5B). The same measurements were performed with MIP26 (100–200 μM), where one tryptophan is exposed to the aqueous environment and neither water nor methyl glucose should have preferential access to the tryptophans. The ratio of SPR signal for MIP26 with ^3H_2O versus ^{3}H-OMG was 0.99 $\pm$ 0.02 ($n = 2$). For comparison, SPR measurements were made using ^3H_2O and ^{3}H-OMG on a solution of *d*-tryptophan (1.4 mM) in 10 mM phosphate buffer. The ratio ($\pm$SE) of the tryptophan SPR signal obtained with ^3H_2O versus ^{3}H-OMG was 1.10 $\pm$ 0.06 ($n = 3$). The SPR ratio for CHIP28 was significantly greater than unity ($p = 0.05$) consistent with the presence of an aqueous pore. The slightly larger (but not statistically significant) SPR signal observed for excitation of tryptophan by ^3H_2O may result from a closer approach (by ca. 3 Å) of ^{3}H to the fluorophore by the smaller ^3H_2O molecule compared to ^{3}HOMG. This closer approach of ^3H_2O would have less effect on the SPR signal for the larger MIP26 (MW = 26000) and CHIP28 (MW = 28000) molecules where most of the fluorescence arises from tryptophans already far from the aqueous compartment.

4. Discussion

The purpose of this study was to investigate whether the single photon radioluminescence arising from tryptophan residues in proteins is measurable and could be exploited to probe tryptophan environment. The SPR method utilizes the energy deposited by a slowing beta decay electron to excite a reporter fluorophore [1]. The small number of emitted radioluminescence photons are detected by a cooled photomultiplier and processed by single photon electronics and pulse-height discrimination. The SPR signal intensity depends upon the molar absorbance and quantum yield of the fluorophore and the distance between the radioisotope and fluorophore. SPR has been applied in studies which do not depend on exact radioisotope–fluorophore distance, including lipid exchange kinetics, membrane transport, and ligand–receptor binding, and in a measurement of the submicroscopic distance between the erythrocyte

membrane bilayer and its glycocalyx [2]. The present study extends the SPR method to the detection of ^3H_2O and other molecules near tryptophan residues in proteins. The theoretical considerations and experimental results in simple proteins indicate that tryptophan radioluminescence is measurable and can be utilized to study tryptophan–water proximity.

A conclusion from our previous work was that for substantial distance from a ^3H source (> 10 nm), the probability of fluorophore excitation increased linearly with the density of energy (keV/cm^3) deposited by a beta electron in the vicinity of the fluorophore [1]. The relationship between energy density and distance from the radioisotope was determined by a Monte Carlo calculation in which the interaction physics of an electron moving through a biological/aqueous environment was modeled. The calculation incorporated the energy distribution of electrons by a specified beta-emitting radioisotope (^3H, ^{14}C or ^{35}S), the energy-dependent deposition of electron energy, and the 3-dimensional trajectory of the electron as it interacts with matter. The present study was focused on energy deposition very near a ^3H source. Although non-zero energy density was found beyond 1 μm for beta electrons from ^3H, a substantial fraction of energy was deposited near the ^3H molecule because of: (a) the $1/r^2$ factor for an isotropically emitting point source, (b) the presence of electrons with low initial energy that interact strongly with matter [9], (c) the non-linear relationship between dipole excitation cross-section and electron energy, and (d) the energy released by electron recombination with the $^3He^+$ produced by beta decay. Although uncertainties in the physics of interaction of low-energy electrons with the medium precluded exact calculation of energy deposition at very small distances (see *Results*), the theoretical considerations described in *Results* suggested that a substantial probability for fluorophore excitation exists in the immediate vicinity of the ^3H molecule. To investigate whether the energy deposited very near the radioisotope could excite tryptophan radioluminescence, SPR measurements were carried out in several model systems.

The very small SPR signals arising from tryptophan residues and the substantial background signal required special attention in the design of experimental protocols and instrumentation. A sample compartment with reflective ellipsoidal optics was designed and constructed to collect the radioluminescence photons efficiently, and to facilitate the safe and precise handling of radioactive samples in a dark room. The collected radioluminescence was detected by a cooled photomultiplier, amplified and quantified by photon counting after exclusion of low- and high-amplitude pulses by multichannel analysis. Measurements were carried out in a Faraday cage in a dark, air-conditioned/dehumidified room. The sources of background signal were: (a) photomultiplier dark current, (b) Bremsstrahlung (stopping radiation), and for the membrane protein samples, (c) weak chemiluminescence. The effects of photomultiplier dark noise were minimized by maximum cooling of a high gain, low-noise photomultiplier, and the use of relatively large amounts of radioactivity (50--200 μCi ^3H per sample) to increase signal intensity. The effects of broad-spectrum Bremsstrahlung were minimized by use of relatively high protein concentrations (20–130 μM) and a UV-passing filter to exclude Bremsstrahlung photons outside the tryptophan emission band.

The soluble protein melittin contains a single tryptophan residue (W17). When dissolved in a low ionic strength buffer (low salt), melittin remains as monomers with an 88% random coil configuration in which the tryptophan is located in a polar environment at the protein–aqueous interface [17]. In a high ionic strength buffer, melittin forms tetramers in which the tryptophan residues are buried in a hydrophobic environment near the center of four monomers. This interpretation was supported by spectroscopic data (Fig. 3A). Based on an α-helical secondary structure for melittin subunits in the tetramer, the average distance between the tryptophan residue and the bulk-phase water compartment is estimated to be ca. 1.5 nm. The experimental data here indicate that the tryptophan SPR signal arising from ^3H_2O decay, after corrections for melittin quantum yield, is 2.0 $\pm$ 0.3-fold higher for identical concentrations of melittin in low versus high salt. This observation is consistent with the exclusion of ^3H_2O from a region near the buried tryptophan residues.

The water soluble tetrameric protein aldolase contains 3 tryptophans (W147, W295 and W313) and 11 tyrosines in each of its monomers. In non-denaturing

sodium phosphate buffer, these fluorescent residues are isolated from the aqueous environment as shown by spectroscopic (Fig. 4A) and I^- quenching (Fig. 4B) data. A fraction of the fluorescent residues are exposed to the aqueous environment (and to ^3H_2O) under denaturing conditions of 8 M urea, giving a 53% rise in SPR signal. Emission spectra from tryptophan/tyrosine excitation (280 nm) and tryptophan excitation (295 nm) showed no difference in peak position, suggesting that the majority of the fluorescence for non-denatured and denatured aldolase arises from the tryptophan residues; however, the number of tryptophans in aldolase precludes assignment of a specific tritium–tryptophan distance or absolute correction for tryptophan quantum yield. Correction for intrinsic differences in the fluorescence intensity of native and denatured aldolase (quantum yield, tyrosine emission, spectral shifts) was made using integrated excitation spectra measured by cuvette fluorimetry. However, absolute values for the SPR signal are not easily interpretable because the SPR excitation cross-section for the fluorophores is not constant in different proteins. Nonetheless, the SPR data provide further evidence for exclusion of water (^3H_2O) from buried tryptophans in native aldolase and increased tryptophan exposure after denaturation by urea.

SPR results comparing fluorophore accessibility to ^3H_2O in different proteins (monellin, HSA, and aldolase) suggest that the cross-section for SPR excitation is greater for protein fluorophores than for monomeric tryptophan or tyrosine in aqueous solution. This effect may involve deposition of energy in or near the protein by the β-particle followed by energy propagation to fluorophores along the covalently linked protein backbone. This mechanism is similar to that described in radiation inactivation, where catalytic sites in proteins are inactivated by a radiation 'hit' anywhere in the protein molecule [28]. Target sizes for such radiation damage measured in frozen samples correlate closely with the molecular size of the protein. Here, the SPR signal produced by the β-particle is likely a result of fluorophore excitation by direct interaction, by ionized water, and by energy propagation along the protein backbone. Therefore, SPR assessment of protein fluorophore exposure to the aqueous environment should only be done for the same protein with changing conditions (e.g. native versus denatured, monomeric versus oligomeric).

CHIP28 is a 28 kDa, water-selective transporting protein that has been isolated and cloned from erythrocytes [21] and kidney [22], and has been shown to transport water in reconstituted proteoliposomes [23,24], stably-transfected CHO cells [25] and *Xenopus* oocytes [26,22]. CHIP28 forms tetramers in membranes [21,27] in which individual monomers function independently [29] and have been proposed to contain a continuously open, narrow aqueous channel. CHIP28 is a member of a family of proteins that includes MIP26 and several small proteins from mammals, plants, bacteria and yeast [30]. MIP26 is a 26 kDa protein from mammalian lens fiber that is homologous to CHIP28 but does not transport water [14]. Fluorescence spectroscopy studies indicate that the four tryptophan residues of CHIP28 (W11, W210, W213, W245) are located in a relatively non-polar environment near the surface and center of the bilayer [20]; in MIP26, one of five (W2, W10, W34, W102, W105) tryptophan residues (W2) lies in a polar environment near the N-terminus.

The data reported here indicate a small, but significantly greater SPR signal for excitation of CHIP28 tryptophan radioluminescence by ^3H_2O than by ^3H-OMG under conditions in which there was no difference in MIP26 tryptophan radioluminescence. The increased signal in CHIP28 in the presence of ^3H_2O is consistent with the conclusion that CHIP28 contains an aqueous channel that admits water but excludes other small molecules including glucose. These results are in agreement with the low single channel water permeability of CHIP28 (suggesting a narrow channel), the inability of CHIP28 to transport urea, protons and small ions [23,22], and lack of water transporting activity of MIP26 [14]. Although the number of water molecules in the CHIP28 aqueous channel and the position of the tryptophans cannot be determined because of the complexity of the protein and the lack of a quantitative model for tryptophan excitation by nearby ^3H_2O molecules, the data demonstrate the utility of tryptophan radioluminescence for detection of intramolecular aqueous compartments.

In summary, the data reported here demonstrate the utility of SPR for detection of ^3H-labeled molecules very near fluorophores in biological sam-

ples. Notwithstanding the relatively large amount of radioactivity and protein samples required to obtain adequate SPR signals, SPR offers a novel approach to probe aqueous environments in proteins.

Acknowledgements

We thank Drs. Stephen Seltzer, Lucas Christophoru, Robert Hamm and Aloke Chatterjee for advice and discussions about the interaction physics of low-energy electrons with matter. This work was supported by grants DK43840, DK27045 and DK35124 from the NIH. Dr. Bicknese was supported in part by NRSA grant GM15145.

References

[1] S. Bicknese, Z. Shahrokh, S.B. Shohet and A.S. Verkman, Biophys. J., 63 (1992) 1256–1266.
[2] Z. Shahrokh, S. Bicknese, S.B. Shohet and A.S. Verkman, Biophys. J., 63 (1992) 1267–1279.
[3] M.R. Eftink and C.A. Ghiron, Anal. Biochem., 114 (1981) 199–227.
[4] B.C. Hill, P.M. Horowitz and N.C. Robinson, Biochemistry, 25 (1986) 2287–2292.
[5] R.C. Chatelier, P.J. Rogers, K.P. Ghiggino and W.H. Sawyer, Biochim. Biophys. Acta, 776 (1984) 75–82.
[6] A.M. Kleinfeld and M.F. Lukacovic, Biochemistry, 24 (1985) 1883–1890.
[7] M.J. Berger and S.M. Seltzer, Tables of Energy-Deposition Distributions in Water Phantoms irradiated by Point-Monodirectional Electron Beams with Energies from 1 to 60 MeV, and Application to Broad Beams, NBSIR Publication 82-2451, National Bureau of Standards, 1982, pp. 1–54.
[8] H. Bethe and J. Ashkin, in E. Segre (Editor), Experimental Nuclear Physics, John Wiley, New York, 1953, pp. 166–357.
[9] M. Mladjenovic, Radioisotope and Radiation Physics, Academic Press, New York, 1973, pp. 124–125.
[10] M. Berger, Improved Point Kernels for Electron and Beta-Ray Dosimetry, NBSIR Publication 73-107, National Bureau of Standards, 1973, pp. 1–20.
[11] C.H. Blanchard and U. Fano, Phys. Rev., 82 (1951) 767.
[12] G.R. Freeman, Kinetics of Non-homogeneous Processes, John Wiley, New York, 1987, pp. 106–124, 172.
[13] J.H. O'Donnell and D.F. Sangster, Principles of Radiation Chemistry, Elsevier, New York, 1970, p. 17.
[14] A.N. van Hoek, M. Wiener, S. Bicknese, L. Miercke, J. Biwersi and A.S. Verkman, Biochemistry, 32 (1993) 11847–11856.
[15] D.E. Gerhart, J. Chem. Phys., 62 (1975) 821–832.
[16] S. Georghiou, M. Thompson and A.K. Mukhopadhyay, Biochim. Biophys. Acta, 688 (1982) 441–452.
[17] J.C. Talbot, J. de Bony Dufourcq, J.F. Faucon and C. Lussan, FEBS Lett., 102 (1979) 191–193.
[18] A.A. Malek, M. Hy, A. Honegger, K. Rose and O. Brenner-Holzach, Arch. Biochem. Biophys., 266 (1988) 10–31.
[19] G. Krishnan and W. Altekar, Biochemistry, 32 (1993) 791–798.
[20] J. Farinas, A.N. van Hoek, L.B. Shi, C. Erickson and A.S. Verkman, Biochemistry, 32 (1993) 11857–11864.
[21] B.L. Smith and P. Agre, J. Biol. Chem., 266 (1991) 6407–6415.
[22] R. Zhang, W. Skach, H. Hasegawa, A.N. van Hoek and A.S. Verkman, J. Cell Biol., 120 (1993) 359–369.
[23] A.N. van Hoek and A.S. Verkman, J. Biol. Chem., 267 (1992) 18267–18269.
[24] M.L. Zeidel, S.V. Ambudkar, B.L. Smith and P. Agre, Biochemistry, 31 (1992) 7436–7440.
[25] T. Ma, A. Frigeri, S.T. Tsai, J.M. Verbavatz and A.S. Verkman, J. Biol. Chem., 268 (1993) 22756–22764.
[26] G.M. Preston, T.P. Carroll, W.B. Guggino and P. Agre, Science, 256 (1992) 385–387.
[27] J.M. Verbavatz, D. Brown, I. Valenti, I. Sabolic, T. Ma, A.N. van Hoek and A.S. Verkman, J. Cell Biol., 123 (1993) 605–618.
[28] E.S. Kempner and A.S. Verkman, Radiat. Phys. Chem., 32 (1988) 341–347.
[29] L.B. Shi, W. Skach and A.S. Verkman, J. Biol. Chem., 269 (1994) 10417–10422.
[30] G.J. Wistow, M.M. Pisano and A.B. Chepelinsky, Trends Biochem. Sci., 16 (1991) 170–171.